1976

Development of a non-destructive inspection technique for advanced composite materials using cholesteric liquid crystals.

Schaum, Robert Troy

Monterey, California. Naval Postgraduate School

DEVELOPMENT OF A NON-DESTRUCTIVE INSPECTION TECHNIQUE FOR ADVANCED COMPOSITE MATERIALS USING CHOLESTERIC LIQUID CRYSTALS

Robert Troy Schaum

NAVAL POSTGRADUATE SCHOOL
Monterey, California

THESIS

Development of a Non-destructive Inspection Technique for Advanced Composite Materials Using Cholesteric Liquid Crystals

by

Robert Troy Schaum

September 1976

Thesis Advisor: M. H. Bank

REPORT DOCUMENTATION PAGE

READ INSTRUCTIONS BEFORE COMPLETING FORM

1. REPORT NUMBER

2. GOVT ACCESSION NO.

3. RECIPIENT'S CATALOG NUMBER

4. TITLE (and Subtitle)
Development of a Non-destructive Inspection Technique for Advanced Composite Materials Using Cholesteric Liquid Crystals

5. TYPE OF REPORT & PERIOD COVERED
Master's Thesis
September 1976

6. PERFORMING ORG. REPORT NUMBER

7. AUTHOR(s)
Robert Troy Schaum

8. CONTRACT OR GRANT NUMBER(s)

9. PERFORMING ORGANIZATION NAME AND ADDRESS
Naval Postgraduate School
Monterey, California 93940

10. PROGRAM ELEMENT, PROJECT, TASK AREA & WORK UNIT NUMBERS

11. CONTROLLING OFFICE NAME AND ADDRESS
Naval Postgraduate School
Monterey, California 93940

12. REPORT DATE
September 1976

13. NUMBER OF PAGES
64

14. MONITORING AGENCY NAME & ADDRESS(if different from Controlling Office)

15. SECURITY CLASS. (of this report)
Unclassified

15a. DECLASSIFICATION/DOWNGRADING SCHEDULE

16. DISTRIBUTION STATEMENT (of this Report)
Approved for public release; distribution unlimited.

17. DISTRIBUTION STATEMENT (of the abstract entered in Block 20, if different from Report)

18. SUPPLEMENTARY NOTES

19. KEY WORDS (Continue on reverse side if necessary and identify by block number)
non-destructive inspection
composite materials
cholesteric liquid crystals

20. ABSTRACT (Continue on reverse side if necessary and identify by block number)

A new, relatively simple and inexpensive non-destructive inspection technique for advanced composite materials is proposed and its feasibility is demonstrated. This technique uses encapsulated cholesteric liquid crystals to sense small temperature differences which result from nonuniform heat transfer through composites. Discontinuities in heat transfer evidenced by

20. (continued)

contrasting surface color patterns indicate material discontinuities, i.e. flaws.

Preliminary investigations into the thermal conductivity of a .041 in. thick graphite/epoxy laminated panel in the direction normal to the composite laminae and in the direction parallel to the laminae are described. The coefficients of conductivity in the two directions were found to differ by an order of magnitude. A qualitative test of the technique in locating embedded teflon triangles is reported, and a design for a testing device is proposed.

DEVELOPMENT OF A NON-DESTRUCTIVE INSPECTION TECHNIQUE FOR ADVANCED COMPOSITE MATERIALS USING CHOLESTERIC LIQUID CRYSTALS

by

Robert Troy Schaum
Lieutenant, United States Navy
B.A.E., Auburn University, 1969

Submitted in partial fulfillment of the
requirements for the degree of

MASTER OF SCIENCE IN AERONAUTICAL ENGINEERING

from the

NAVAL POSTGRADUATE SCHOOL

September 1976

ABSTRACT

A new, relatively simple and inexpensive non-destructive inspection technique for advanced composite materials is proposed and its feasibility is demonstrated. This technique uses encapsulated cholesteric liquid crystals to sense small temperature differences which result from nonuniform heat transfer through composites. Discontinuities in heat transfer evidenced by contrasting surface color patterns indicate material discontinuities, i.e. flaws.

Preliminary investigations into the thermal conductivity of a .041 in. thick graphite/epoxy laminated panel in the direction normal to the composite laminae and in the direction parallel to the laminae are described. The coefficients of conductivity in the two directions were found to differ by an order of magnitude. A qualitative test of the technique in locating embedded teflon triangles is reported, and a design for a testing device is proposed.

TABLE OF CONTENTS

LIST OF FIGURES

LIST OF SYMBOLS

A	the cross-sectional area of a fin or wall through which heat flow is examined -- ft^2
C	the circumference of a cross section at a location along the length of a fin -- ft
H	a constant -- h_e/km -- Nondimensional
h	lateral fin surface film coefficient -- BTU/h ft^2 ^oF
h_c	thermal contact coefficient -- BTU/h ft^2 ^oF
h_e	film coefficient at fin end -- BTU/h ft^2 ^oF
k	thermal conductivity -- BTU/h ft ^oF
k_{mn}	thermal conductivity of material between planes m and n -- BTU/h ft ^oF
L	fin length measured perpendicular to the major surface of attachment -- ft
m	a constant -- the square root of hC/kA -- ft^{-1}
q	rate of heat flow through a material -- BTU/h
t	temperature -- ^oF or ^oC
t_f	temperature of the bulk of ambient fluid -- ^oF or ^oC
t_n	temperature at location n -- ^oF or ^oC
t_o	fixed temperatute at the fin base -- ^oF or ^oC
x	coordinate along the length of the fin -- ft or in
Δx	material thickness -- ft or in
Δx_{mn}	material thickness between planes m and n -- ft or in
θ	temperature difference between a point in a material and the ambient fluid -- ^oF or ^oC
θ_o	temperature difference between fin base temperature and the ambient fluid -- ^oF or ^oC
$1/h_c A$	thermal contact resistance -- h ^oF/BTU

I. INTRODUCTION

Since the early development of boron/epoxy and graphite/epoxy composite laminates it has been recognized that non-destructive testing techniques developed for use in metalic structures are often inadequate for composites. An effort to obtain effective non-destructive testing techniques has resulted in the development of a number of moderately successful methods. These techniques include ultrasonic, radiographic, sonic, infrared, thermochromic, photochromic, holographic interferometry, dye penetrant and hardness tests, and are discussed in Refs. 1 and 2. Although each method has its unique advantages and disadvantages, they generally share a high level of sophistication and complexity and frequently enjoy only limited laboratory use. It is not surprising, therefore, that a simple yet effective non-destructive testing technique is desired which can be inexpensively and easily performed by personnel with limited technical training.

In recent years some potentially effective ultrasonic and holographic techniques have been devised (Ref. 3) and the use of a relatively compact mobile holographic non-destructive testing device has been demonstrated (Refs. 4 and 5). Among the simplest are those developed in the latter part of the 1960's which involve the use of cholesteric liquid crystals in thermal mapping. Some applications of these methods are presented in Refs. 6 and 7, including the location of interlaminar electrical shorts in electronic circuit boards, the prediction of fatigue and fracture locations, crack detection and the inspection of adhesively bonded

structures. Brilliant color patterns can be observed through the application of liquid crystals to a few square feet of a surface which exibits nonuniform temperatures. Their use is particularly desirable when the temperature variation can be attributed to nonuniform heat transfer through a material containing some nonhomogeneity or discontinuity. Two problems that hindered the early use of cholesteric liquid crystals in large-scale non-destructive testing are the short useful lifetime of pure cholesteric liquid crystals and the expense of coating large objects. The following development of a non-destructive technique for detecting discontinuities and nonhomogeneities in advanced composite plates addressed the problem of coating large areas.

Three separate stages in the development of a proposed compact, mobile device were completed. First was the determination of the coefficient of thermal conductivity normal to the layers of a graphite/epoxy panel. Second was the determination of the coefficient of conductivity parallel to layers. References 8 and 9 provided the theoretical background for a steady state analysis of heat transfer in the laminate. When order-of-magnitude values for the two coefficients of conductivity had been obtained, the third stage was begun. It involved the actual test of a 14 x 14 in. graphite/epoxy panel containing intentionally embedded nonhomogeneities. Ultimately the final device was conceptually designed and partially constructed. Key to the design was the procurement of a thin (.005 in.) mylar-insulated foil heater 6 in. square.

As previously mentioned, pure liquid crystals, while exibiting brilliant colors, deterorate rapidly once applied to a surface and provide only a few hours for viewing and experimentation. A brief discussion of liquid crystals including encapsulated cholesteric liquid crystals (the type actually used in the work hereinafter described) is

appropriate.

1. Cholesteric Liquid Crystals

Detailed information concerning the origin, composition and uses of liquid crystals can be found in Refs. 10, 11 and 12, and is summarized here. In the latter part of the 19th and early 20th centuries, scientists such as Friedrich Reinitzer began work on selected organic compounds that, in the thermal transformation from solid to liquid state, passed through an intermediate phase which exibited the anisotropic optical properties of crystalline solids. Subsequent research concerning the structure of liquid crystals resulted in classification of liquid crystals into one of three categories: smetic, nematic, or cholesteric, the category being determined by the particular molecular arrangement of the liquid crystals.

The response of cholesteric liquid crystals to thermal variations makes them an important tool for the acquisition of both quantitative and qualitative information in laminate heat transfer problems. A particular formulation of specific cholesterol esters will provide liquid crystals that exibit a reversible and repeatable response to temperature of a given range. The cholesteric liquid crystals respond by sequentially passing through the complete visual spectrum -- red through violet -- in fractions of degrees, or multiples of degrees, depending on the specific formulation. The range is generally referred to as the "event temperature range" or "colorplay range". Since colors scattered by liquid crystals represent only a fraction of the incident light (the remainder being transmitted by the liquid crystals), an absorptive black background is needed to prevent reflection of the transmitted light.

Many of the problems posed by the use of pure cholesteric liquid crystals, including atmospheric contamination and short life, have been greatly reduced by an encapsulation process for packaging labile materials developed by the National Cash Register Company. The encapsulation process coats the liquid crystals with gelatin in a polyvinyl alcohol binder to form tiny packages 2 - 50 microns in diameter. In addition to extending the life of the liquid crystals to as long as several years by minimizing surface contamination and ultra violet light exposure of the raw liquid crystals, the encapsulation process greatly reduces the variation in color due to viewing angle. The colors remain readily visible, albeit subdued, to the human eye. Encapsulated Liquid Crystals may be obtained in two forms, either precoated on a blackened paper or mylar film, or in a water based slurry. The slurry form was used for spray coating surfaces after thinning, 1 part E.L.C. and 2 parts water, with the addition of 2 drops of Kodak Photoflo solution to 2 oz. of the mixture to improve surface wetting.

Encapsulated Liquid Crystals may be formulated to respond over a wide range of event temperatures. There are three series represented by E.L.C. nomenclature: S (sensitive), 1.5 $\pm$ 0.5°C colorplay; R (regular), 3.5 $\pm$ 1.0°C colorplay; W (wide), 6.0 $\pm$ 2.0°C colorplay. The S - series were exclusively used for highest sensitivity; their characteristic event temperatures are listed in Appendix A.

II. HEAT TRANSFER NORMAL TO LAYERS OF A LAMINATE

A. ONE-DIMENSIONAL STEADY STATE HEAT CONDUCTION

"Steady state conduction" is a condition which exists when temperatures of fixed points within a heat-conducting body do not change with time. This also implies that the time rate of heat flow between any two selected points is constant with time. The term "one-dimensional" can be applied to a heat conduction problem when only one space coordinate is necessary to describe the temperature distribution within a heat-conducting body. Although such a situation rarely exists in practice, the one-dimensional condition can be assumed as a close approximation in the study of heat flow normal to the surface of the graphite/epoxy laminate. The heat flow through a plane wall, at regions sufficiently removed from the edges, depends only on the coordinate measured normal to the plane of the wall. By insulating a finite wall at its edges one may neglect edge effects and a practical one-dimensional heat conduction problem exists.

The elementary heat conduction problem of a plane wall of finite thickness Δx but infinite in extent (to allow a one-dimensional assumption) with each face maintained at a uniform temperature is represented by Eq. 2.1 (Ref. 8).

$$\frac{q}{A} = k \frac{t_1 - t_2}{x_2 - x_1} = k \frac{t_1 - t_2}{\Delta x_{12}} \qquad (2.1)$$

The above expression is written in terms of q/A, the rate of

heat flow per unit area, Δx, the wall thickness, and the respective uniform face temperatures, t_1 and t_2, for a material having thermal conductivity k.

Now consider the more general plane wall, illustrated in Fig. 1(a), composed of three layers (although any number could have been used) each of different thickness and thermal conductivity. Denote each juncture of two different materials by a number 1 through 4 and adopt the following notation:

- Δx_{mn} = thickness between planes m and n
- k_{mn} = thermal conductivity of material between planes m and n

If the outside temperatures, t_1 and t_4, are specified and the individual material thicknesses and thermal conductivities are known, then the temperature distribution through the wall and rate of heat flow can be calculated. Since the steady state condition is assumed to exist and since the rate of heat flow per unit area q/A, is constant, Eq. (2.1) may be applied to each layer yielding the following:

$$\frac{q}{A} = \frac{t_1 - t_2}{\Delta x_{12}/k_{12}} = \frac{t_2 - t_3}{\Delta x_{23}/k_{23}} = \frac{t_3 - t_4}{\Delta x_{34}/k_{34}} \qquad (2.2)$$

Solving for the individual temperature differences and then eliminating the unknown temperatures the expression, Eq. (2.3), for heat flow through the wall in terms of overall temperature difference is obtained.

$$\frac{q}{A} = \frac{t_1 - t_4}{\frac{\Delta x_{12}}{k_{12}} + \frac{\Delta x_{23}}{k_{23}} + \frac{\Delta x_{34}}{k_{34}}} \qquad (2.3)$$

Next consider a practical modification to the "infinite

slab" (the wall with no edge effects) problem just discussed. By extracting a small circular section normal to the plane of the wall in Fig. 1(a) and insulating it, the one-dimensional problem can be preserved, with the assumption that although edge effects may now exist, they are small. The practical problem now depicted in Fig. 1(b) is one of two insulated circular cylinders of the same material sandwiching a thinner dissimilar disc.

1. Contact Resistance

Imagine two solid rods brought into contact as indicated in Fig. 2(a), with sides insulated so that heat flows only in the axial direction. The materials may have different thermal conductivities, but if their sides are insulated the heat flux must be the same through both materials under the steady state conditions. Experience has shown that the actual temperature profile through the materials varies approximately as shown in Fig. 2(b). The temperature drop at plane 2 is caused by thermal contact resistance. The physical mechanism of contact resistance may be better understood by close examination of the joint in detail. No real surface is perfectly smooth and the actual surface roughness is believed to play a central role in determining the contact resistance. There are two principal contributions to the heat transfer at the joint:

- The solid-to-solid conduction at the spots of contact
- The conduction through entrapped gases in the void spaces created by the contact.

The second factor represents the major resistance to heat flow. The quantity $1/(h_c A)$ is the thermal contact resistance and h_c is the contact coefficient. Including the contact

coefficient in Eq. (2.3) accounts for the thermal contact resistance encountered in the real problem and Eq. (2.4) results.

$$\frac{q}{A} = \frac{t_1 - t_4}{\frac{\Delta x_{12}}{k_{12}} + \frac{\Delta x_{23}}{k_{23}} + \frac{\Delta x_{34}}{k_{34}} + \frac{1}{h_{c_{23}}} + \frac{1}{h_{c_{34}}}} \tag{2.4}$$

Let the materials between planes 1 and 2 and planes 3 and 4 be the same and their thicknesses x_{12} and x_{34} be equal. Further, if the surfaces of contact at planes 2 and 3 have equal roughness characteristics, one may combine the contact coefficients and Eq. (2.4) can be simplified as follows:

$$\frac{q}{A} = \frac{t_1 - t_4}{\frac{2\Delta x_{12}}{k_{12}} + \frac{\Delta x_{23}}{k_{23}} + \frac{1}{h_{c_{24}}}} \tag{2.5}$$

where

$$\frac{1}{h_{c_{24}}} = \frac{1}{h_{c_{23}}} + \frac{1}{h_{c_{34}}} \tag{2.6}$$

Once again considering the experimental problem of the thin disc sandwiched between two circular rods previously discussed and illustrated in Fig. 1(b), q/A may be found using either the first or third of Eqs. (2.2). Further, given the physical dimensions of the two rods and the disc as well as their respective thermal conductivities, the contact coefficient may be found by solving Eq. (2.5).

Assume that the contact conditions for two discs, one of known thermal conductivity and one of unknown thermal conductivity, can be made equal. The contact coefficient found in the known case may be used in the other case to solve for the unknown thermal conductivity. The problem studied was one in which the thermal conductivity of the graphite/epoxy laminate disc was unknown in addition to the

unknown contact coefficient.

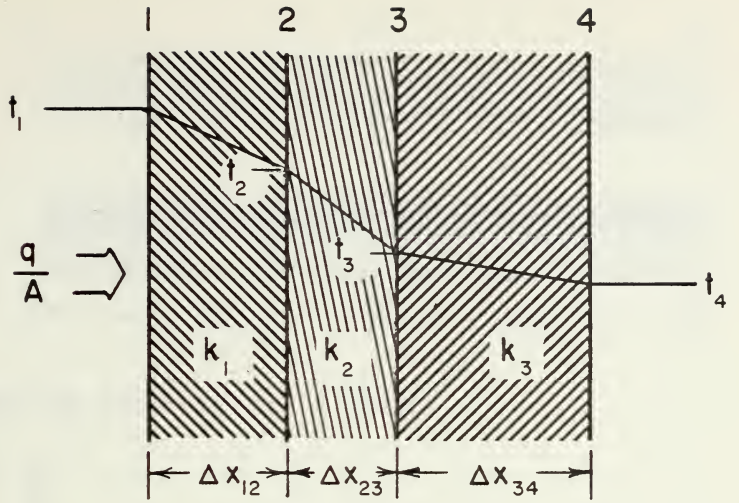

(a) One-dimensional, multilayer wall case

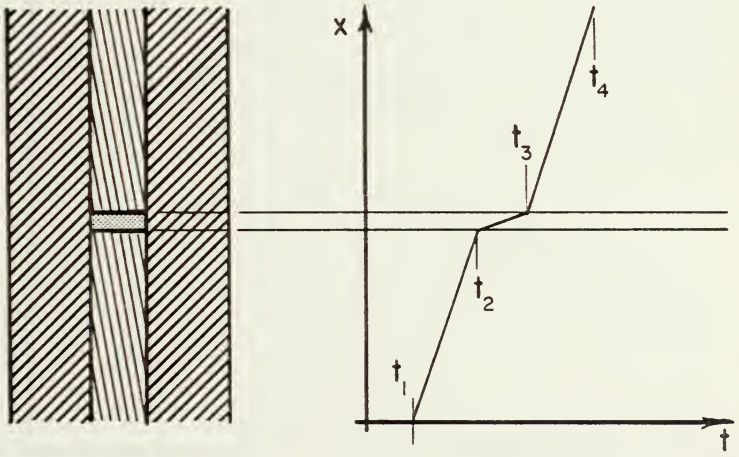

(b) One-dimensional, thin specimen case

Figure 1 - HEAT TRANSFER NORMAL TO THE LAYERS OF A LAMINATE

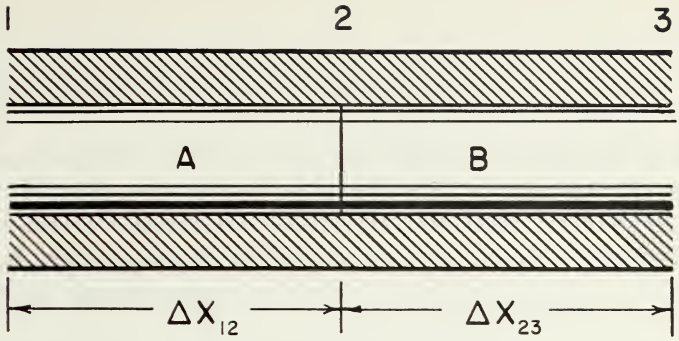

(a) Two insulated solid rods

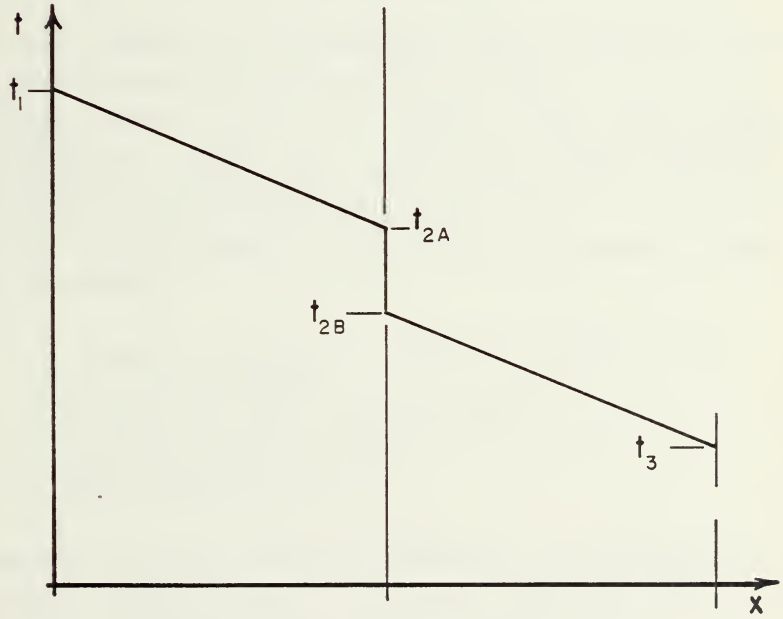

(b) Temperature Profile

Figure 2 - CONTACT RESISTANCE

B. EXPERIMENTAL APPARATUS AND PROCEDURE

The apparatus used for the experimental determination of the coefficient of conductivity normal to the layers of a graphite/epoxy specimen is shown in Figs. 3 and 4. Heat Transfer Unit I, shown in detail in Fig. 3, is composed of three basic components:

1. Bottom boiler -- steam heat source
2. Connecting insulated copper rods
3. Top insulated ice bath -- heat sink

The test section to hold specimen discs is located in the gap formed between the ends of the two rods.

Each copper rod was fitted with four small (approximately .020 in. diameter) copper-constantan thermocouples inserted into holes drilled to the rod center at locations consecutively rotated 90°.

The entire apparatus, shown in Fig. 4, consists of four main components:

1. Voltmeter capable of millivolt output for thermocouple reading
2. 8-position rotary selector switch
3. Ice bath reference point
4. Heat Transfer Unit I

Appendix B contains information regarding the dimensions and thermal conductivities of material specimens used, in addition to properties of other materials used in the construction of the apparatus.

The procedure described below was followed to obtain a practical estimate of the contact coefficient which was used in Eq. (2.5) and ultimately in conjunction with Eq. (2.2) to

find the thermal conductivity normal to the layers of the graphite/epoxy composite. During one testing period nine 3/4 in. diameter specimen discs, six metal and three composite, were examined. Also during each period two test sequences were performed with no specimen to determine the magnitude of the copper-heatsink compound-copper contact coefficient. For all contact surfaces, already with similarly machine finished surfaces, G and C Electronics heatsink compound was used as a thin uniform coating to reduce the effect of air entrapped in surface voids.

Two methods were used in the arrangement of thermocouple output:

- "The direct method," which included an ice bath reference in the thermocouple circuit.
- "The differential method," which eliminated the ice bath by connecting the copper sides of pairs of thermocouples located equidistant from the gap (1 and 8, 2 and 7, 3 and 6, 4 and 5).

The following is a detailed sequence describing one test period:

1. After lightly coating the contact surfaces of one specimen disc with the heatsink compound it was inserted in the gap between the copper rods with boiling water in the bottom container and the ice bath in the top.
2. A 25 lb. weight was placed on top of the ice bath to enhance the release of entrapped air in the contact voids.
3. When the voltmeter output settled indicating that temperatures in the copper rods had stabilized at steady state values, the millivolt output was recorded (using either the pre-wired direct or differential method) using the rotary

switch to sequentially select specific thermocouple circuits.

4. The temperatures (or temperature differences) were plotted versus rod length. A linear polynomial fit and extrapolation were used to determine t_2 and t_3 (or Δt) across the gap. (See Fig. 5 as an example).
5. Steps 3 and 4 were repeated three times for each specimen during each test sequence.
6. Steps 1 through 5 were repeated for all nine specimens and the two previously mentioned "no specimen" sequences were performed to complete an entire test period.

Subsequent data reduction for appropriate temperatures and use of the known thermal conductivities provided solutions to Eq. (2.5) in terms of h_c. The mean of these contact coefficients was then used to compute the thermal conductivity in a direction normal to the layers of the graphite/epoxy specimens.

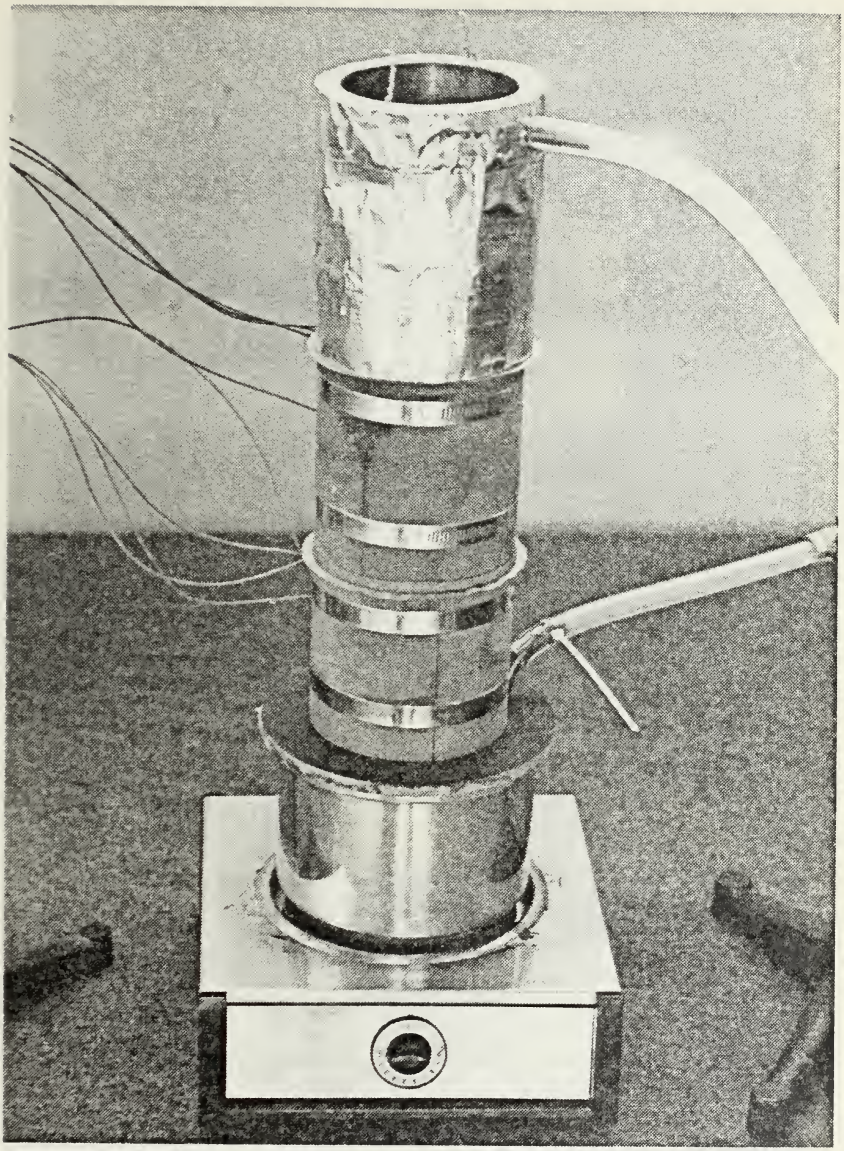

Figure 3 - HEAT TRANSFER UNIT I

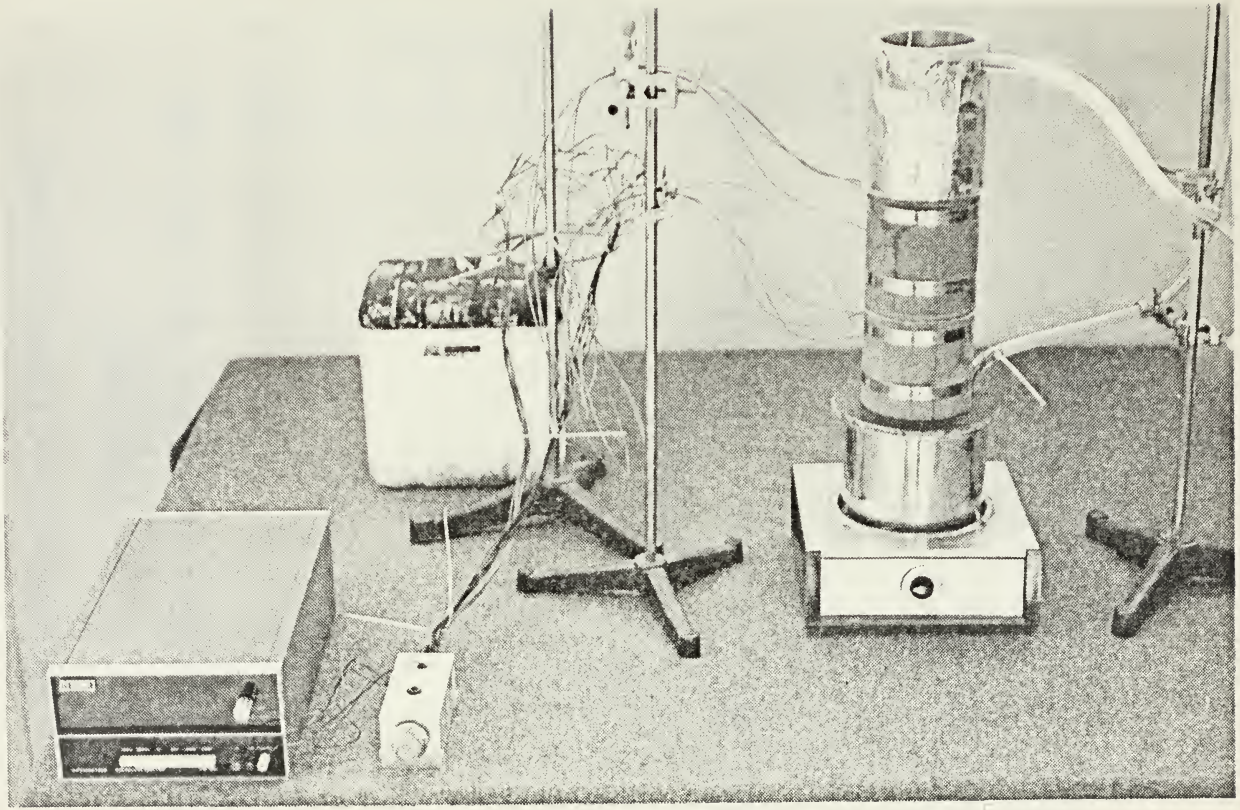

Figure 4 - APPARATUS: HEAT TRANSFER NORMAL TO LAMINATE LAYERS

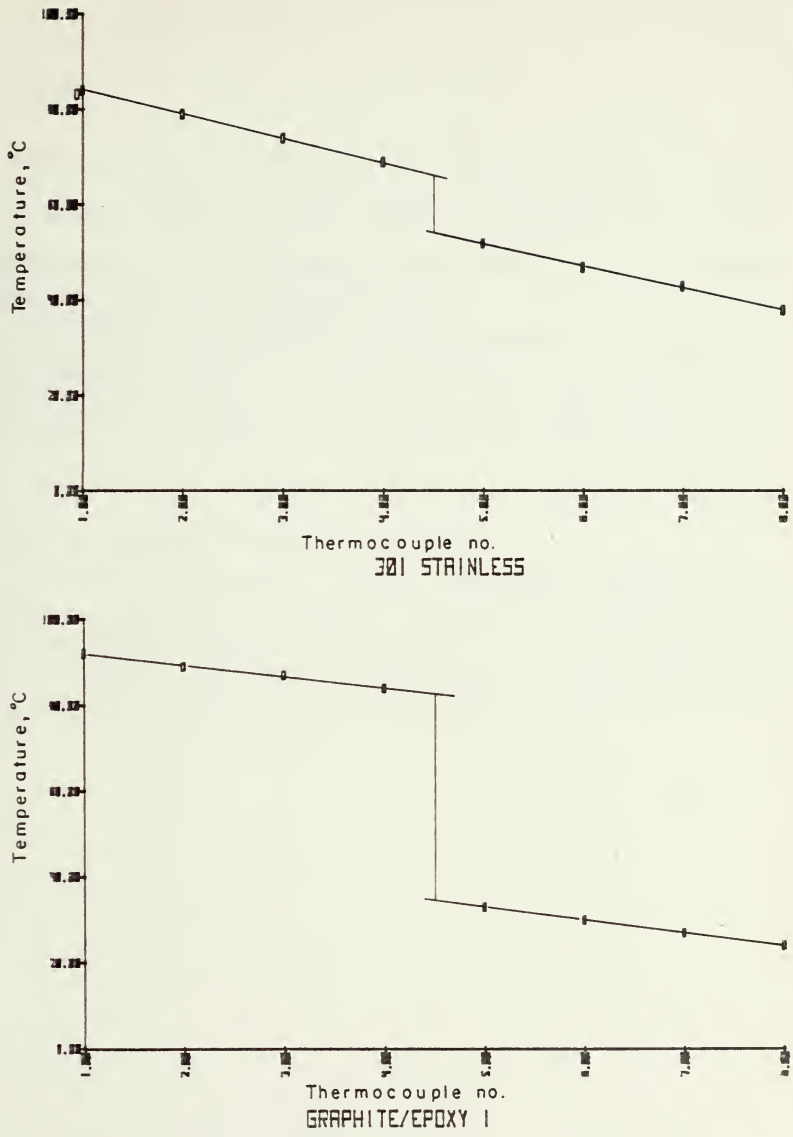

Figure 5 - EXAMPLE Δt FOR TWO SPECIMENS

C. RESULTS

Figure 6 is a summary of the values of $1/h_c$ obtained over three separate test periods displayed for viewing convenience and not to infer a correlation between specimen thickness and contact coefficient.

One of the three graphite/epoxy specimens had smoother surfaces than the other two; therefore, in calculating the coefficient of conductivity using data from the rougher specimens, the value of $1/h_c$ used was increased from the mean by one sample standard deviation to account for the effect of increased surface roughness.

The nine subsequent values for the coefficient of thermal conductivity measured normal to layers in the graphite/epoxy laminate ranged from .534 to.907 BTU/h ft ^{o}F with a sample mean value of .748 BTU/h ft ^{o}F and associated sample standard deviation of .121 BTU/h ft ^{o}F .

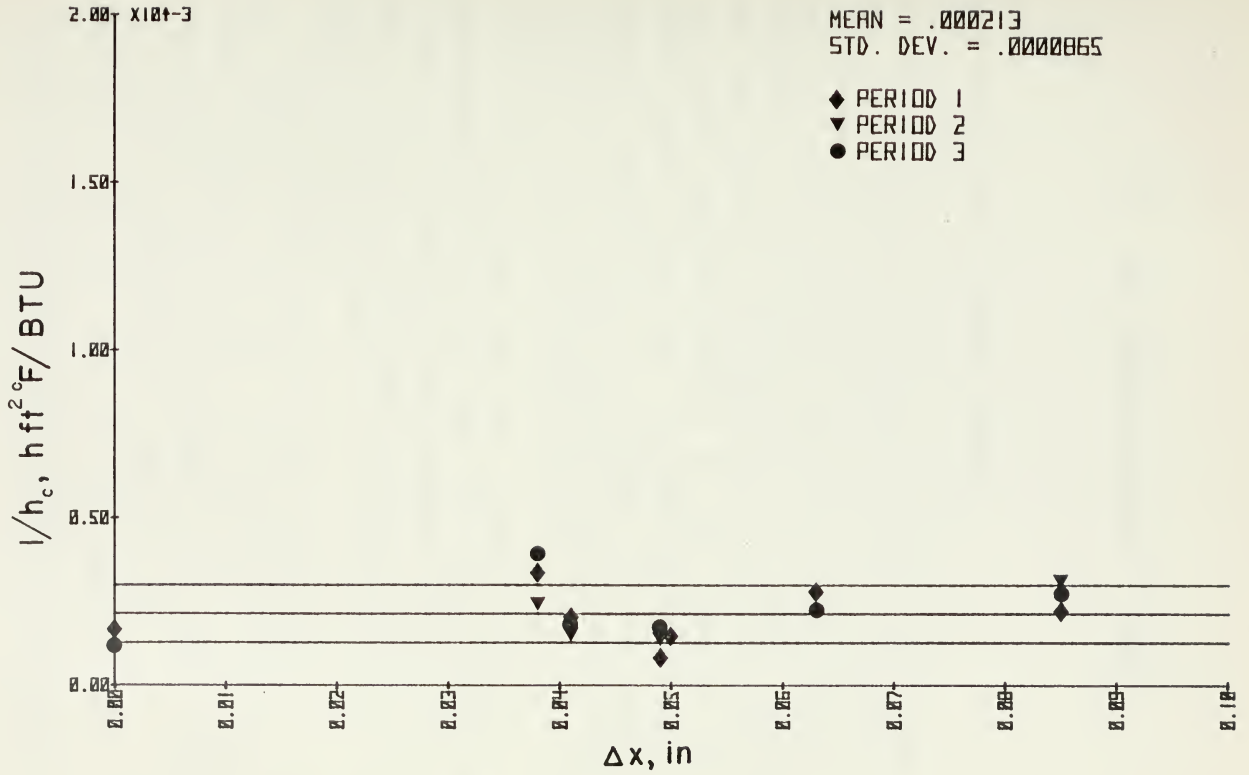

Figure 6 - SUMMARY: SPECIMEN THICKNESS vs. CONTACT COEFFICIENT

III. HEAT TRANSFER PARALLEL TO LAYERS

A. STRAIGHT FIN OF UNIFORM THICKNESS

When examining the inplane heat transfer problem one is led to the study of heat transfer for a thin fin. If the fin proportions used in practice are such that the length of the fin (the dimension measured normal to the primary surface of attachment) is large compared with its maximum thickness, one may assume that the temperature of the fin depends only on a single coordinate measured in the direction of the fin's length. Thus, when the above simplification can be made, the problem for the solution of the temperature distribution and heat flux rate becomes a one-dimensional problem. The following analysis addresses only the steady state case.

For the straight fin of uniform thickness the cross-sectional area for heat flow (normal to the length coordinate) is constant. Also the exposed surface area for heat convection is a linear function of the distance measured along the length; i.e., the perimeter of the cross section is constant.

Figure 7(a) illustrates the fin configuration and shows the notation to be used in the following analysis. The symbol L denotes the length of the fin, k the thermal conductivity, h the film coefficient of the exposed surface, t_o the fixed temperature at the fin base, and t_f the temperature of the bulk of the ambient fluid. The coordinate distance along the fin length is symbolized by x. A and C are used to denote the area of a cross section

normal to x and the perimeter of the section, respectively.

From conservation of energy in the steady state, Fourier's law and the definition of the film coefficient h, one obtains the classic differential equation for the distribution of temperature in the fin (Ref. 8):

$$\frac{d^2t}{dx^2} - \frac{hC}{kA}(t - t_f) = 0 \qquad (3.1)$$

Equation (3.1) must be satisfied at every point in the fin, and if the film coefficient and the thermal conductivity may be assumed constant, it can be easily solved. The equation can be made more concise by defining the following parameters:

$$\theta = t - t_f \qquad (3.2)$$

$$m = \sqrt{\frac{hC}{kA}} \qquad (3.3)$$

Substituting the definitions yields the differential equation, Eq. (3.4).

$$\frac{d^2\theta}{dx^2} - m^2\theta = 0 \qquad (3.4)$$

The general solution to Eq. (3.4) including arbitrary constants B and D found by applying boundary conditions is given by Eq. (3.5).

$$\theta = Be^{-mx} + De^{-mx} \qquad (3.5)$$

For the present let the boundary conditions be those depicted in Fig. 7(a) -- an imposed temperature at the base and convection at the free end. These boundary conditions may be written:

$$\begin{aligned} &\text{At } x=0: \ \theta = \theta_o = t_o - t_f \\ &\text{At } x=L: \ \frac{d\theta}{dx} = -\frac{h_e}{k}\theta \end{aligned} \qquad (3.6)$$

It should be noted that the boundary condition of convection at the end of the fin as stated above permits the film coefficient at the end, h_e, to be different from the film

coefficient on the lateral surfaces, h. Subsequent evaluation of B and D and substitution into the general solution leads to the following expression for the temperature distribution along the fin:

$$\frac{\theta}{\theta_0} = \frac{t - t_f}{t_0 - t_f} = \frac{\cosh m(L-x) + H\sinh m(L-x)}{\cosh mL + H\sinh mL} \qquad (3.7)$$

where

$$H = \frac{h}{\frac{e}{km}} \quad \text{and} \quad m = \sqrt{\frac{hC}{kA}} \qquad (3.8)$$

In the development of Eq. (3.7) it was assumed that the fin was slender enough for a one-dimensional condition to prevail. If this condition is met it is very likely that the heat convected out the end of the fin is a small fraction of the heat convected out the other surfaces. Therefore, Eq. (3.7) may be simplified by neglecting end heat loss. This implies $h_e = 0$, or H=0 and Eq. (3.7) becomes:

$$\frac{\theta}{\theta_0} = \frac{t - t_f}{t_0 - t_f} = \frac{\cosh m(L-x)}{\cosh mL} \qquad (3.9)$$

A major difficulty in using Eq. (3.9) in a practical problem is in the determination of h. The basis for an experimental determination of h is illustrated in Fig. 7(b), in which the temperature distribution along the length of two fins is known as well as their dimensions. If these temperature distributions were derived from the same actual conditions for two fins of identical dimensions, both fins must have the same film coefficient h. By substituting the appropriate known values into Eq. (3.9) for each of the two fins and ratioing the subsequent equations, Eq. (3.10) results.

$$\frac{\theta_1}{\theta_{01}}\frac{\theta_2}{\theta_{02}} = \frac{(t-t_f)_1}{(t-t_f)_2}\frac{(t_0-t_f)_2}{(t_0-t_F)_1} = \frac{\cosh m_1(L-x)_1}{\cosh m_1 L_1}\frac{\cosh m_2 L_2}{\cosh m_2(L-x)_2} \qquad (3.10)$$

Since the only unknown is now h, common to both fins and

found in the terms m_1 and m_2, an iterative solution will yield the actual value of h. Once the actual value of h is known it may be used to solve for an unknown coefficient of thermal conductivity in any other geometrically similar fin sharing the same environment.

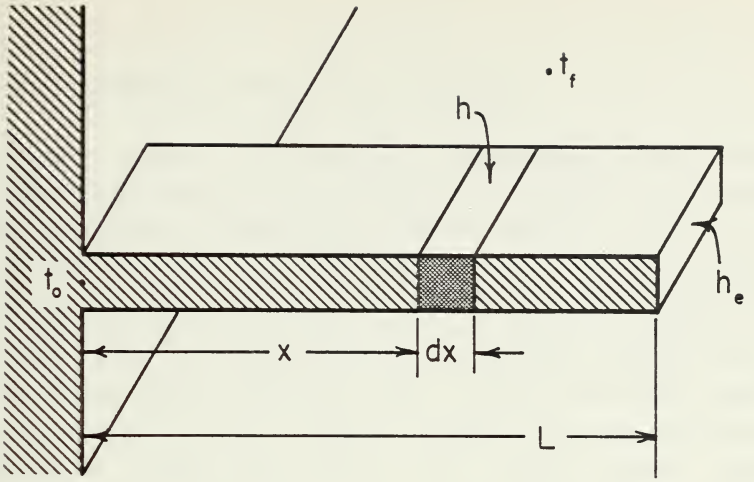

(a) Straight fin of uniform thickness

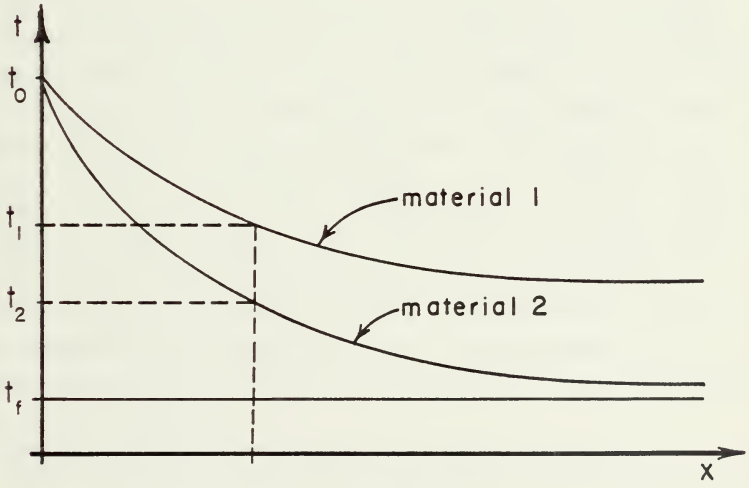

(b) Temperature vs. Length — two fins

Figure 7 - STRAIGHT FINS

B. EXPERIMENTAL APPARATUS AND PROCEDURE

To obtain information concerning the thermal conductivity parallel to layers in samples of specific graphite/epoxy laminates, Heat Transfer Unit II was constructed (Fig. 8). It consists of a rectangular aluminum tank with three tubular threaded portions welded into holes in the tank side wall. Each of the tubular portions was fitted with an open center cap and teflon washer. Six fin units were used; each was a long, narrow, thin fin, inserted into a size no. 9 rubber stopper. For each test period three of these fin units, two with known thermal conductivities and one with unknown thermal conductivity, were placed in the tubular sections and caps tightened to lock the units.

All of the fins were machined as nearly as possible to the same dimensions, and all were prepared for testing in the same manner. A typical fin unit is shown in Fig. 9. The base of each fin, (considered to be the distance from the exterior face of the stopper, through the stopper to the interior of the tubular section of the boiler tank), a distance of 3 in., was coated with a clear plastic varathane. This coating was primarily necessary for the waterproofing of the laminate fins. The portion of the fin exterior to the stopper over which a temperature profile was to be measured was sprayed with flat black enamel. Over the enamel was sprayed a mixture of cholesteric liquid crystals, S-30, S-32, and S-62.

During a single testing period water in the rectangular tank was brought to a boil with the use of an electric hot plate which ultimately provided a steady state temperature base for the fins in well circulated boiling water.

When the color play patterns on the three fins had stabilized, the ambient temperature was recorded and the

positions of the green and blue color zones were marked on each fin as well as the position of the black separation zone between s-30 and s-32 crystals. The position of each mark was measured from the face of the stopper and recorded with the appropriate temperature for the particular color zone. The length of the fin extending from the face of the stopper was also recorded.

From these measurements temperature vs. fin length curves were constructed. Figure 10 is a composite plot of six individual curves found in Appendix C. Incrementing x from 0.5 in. to 2.0 in. in 0.5 in. steps and using corresponding temperatures from fins of known thermal conductivity, a value for h was determined. This value of h was used to calculate a value for k measured parallel to layers in the two laminate fins. A typical representation of these values of thermal conductivity is given in Fig. 11. The value for the thermal conductivity of the graphite/epoxy laminate in a direction parallel to layers was taken to be the average of the values represented in Fig.11 for each test period.

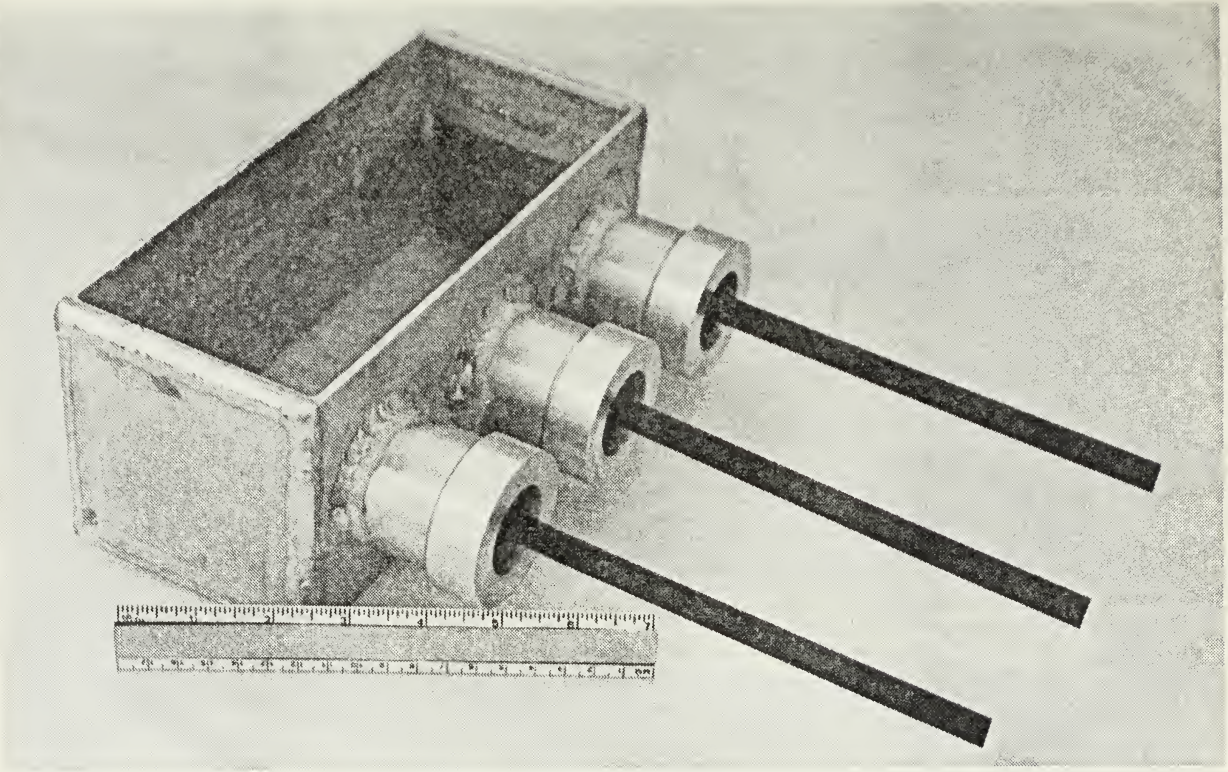

Figure 8 - HEAT TRANSFER UNIT II

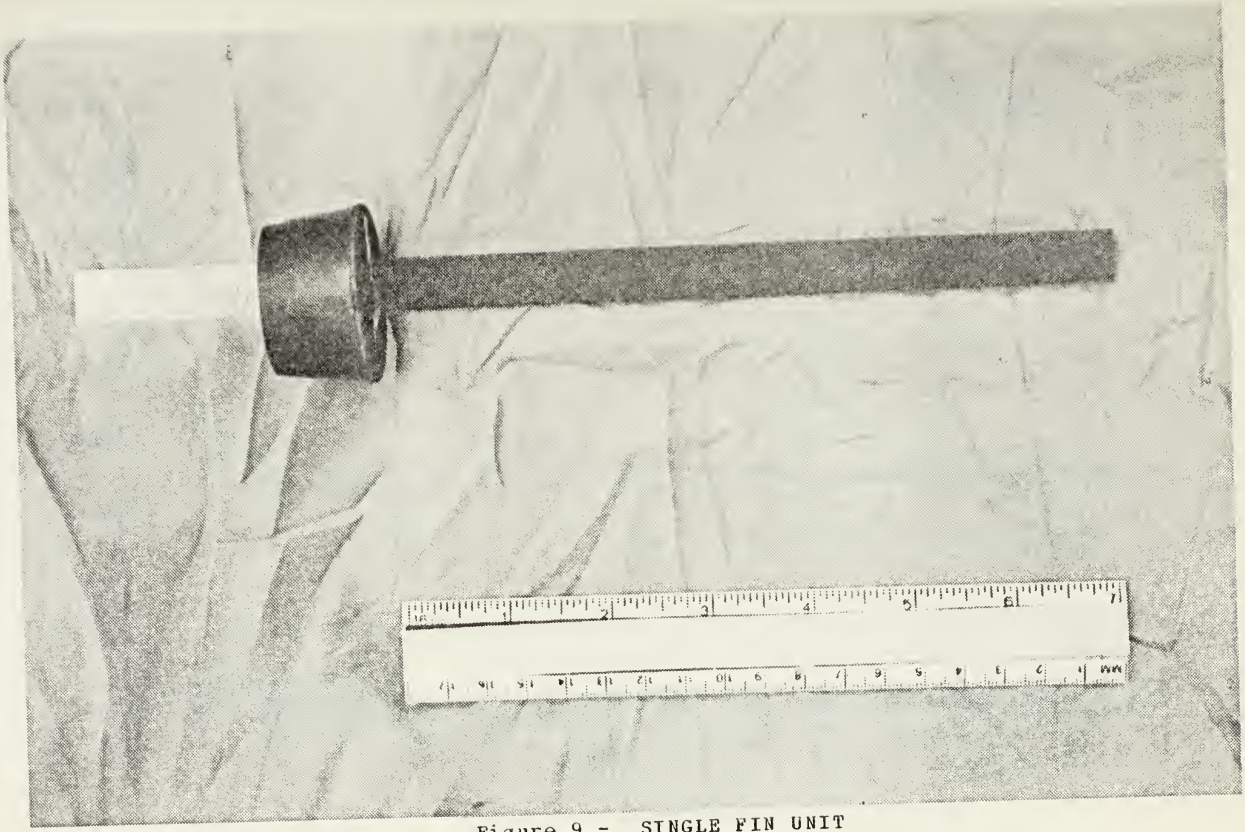

Figure 9 - SINGLE FIN UNIT

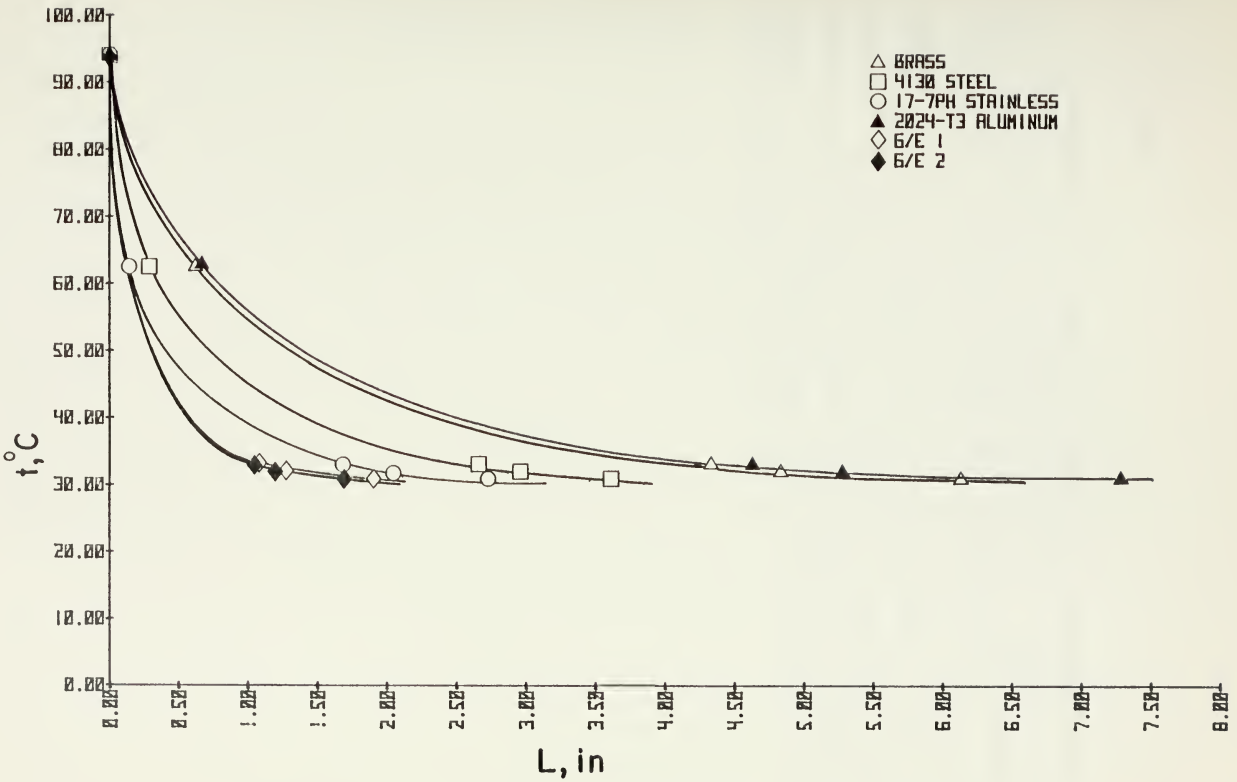

Figure 10 - SUMMARY: TEMPERATURE vs. FIN LENGTH

C. RESULTS

A summary of the resulting values for the coefficient of conductivity in a direction parallel to layers in the graphite/epoxy fins is presented in Fig. 11. The scattered results at 1.5 and 2.0 inches are attributed to $t - t_f$ the sensitivity of the calculations to small values of (Fig. 10) obtained in that region. Including the scattered values, however, still yields a sample mean value for k parallel to layers in the graphite/epoxy fin of 6.61 BTU/h ft ^{o}F with sample mean value of 1.25 BTU/h ft ^{o}F.

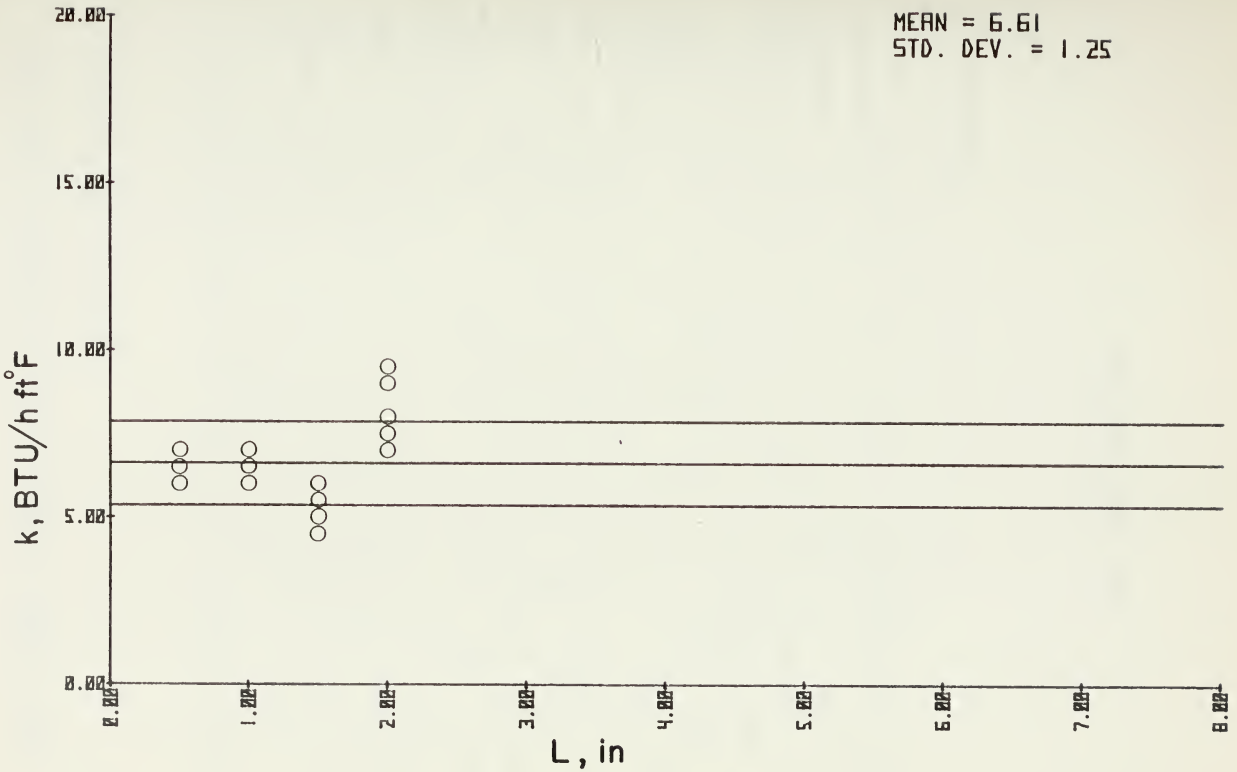

Figure 11 - THERMAL CONDUCTIVITY vs. FIN LENGTH

IV. COMPOSITE TEST PANEL

A. BACKGROUND

With knowledge of the relative magnitudes of thermal conductivities for the specific graphite/epoxy laminates available, the final step before designing an actual flaw detection device was to attempt flaw detection in a graphite/epoxy panel with intentionally embedded flaws.

Recalling the discussion of one-dimensional heat flow through a wall, and observing that the panel could be treated as a thin wall, provides a basis for a non-destructive test of the panel. Consider two paths for heat flow from the rear surface to the front surface of the panel. Let Path 1 pass through only the wall material and Path 2 pass through the wall material as well as through an embedded flaw. By supplying a uniform rear surface temperature and assuming heat flow rate constant, and with the application of Eq. (2.3) to both paths, it can easily be shown that the front surface temperature will be different for the two paths. Is the temperature difference between a surface location above a flaw and a surface location below which no flaw exists sufficient to be detected through the use of encapsulated cholesteric liquid crystals? That is the question addressed in the experiment described below.

B. APPARATUS AND PROCEDURE

An 8-ply $[(0/90)_2]_s$ graphite/epoxy panel, shown in

Fig. 12, was constucted from NARMCO Rigidite 5208-UCC Thornel 300 prepreg tape. Sixteen teflon triangles, shown in detail in Fig. 13, were embedded in the panel as intentional "flaws" or material discontinuities.

Three types of quantitative information regarding the detection sensitivity were desired:

- Flaw width sensitivity information
- Flaw thickness sensitivity information
- Flaw depth location sensitivity information

The area of the triangles and the included angles were selected to facilitate evaluation of the anticipated surface detection pattern. Choosing the three angles such that angles 2 and 3 were twice and four times angle 1, respectively, allowed consideration of three substantially different tapers.

It was anticipated that by comparing the shape of the surface temperature pattern with the known shape of the teflon triangles one could quantitatively determine flaw width sensitivity of the proposed technique. The 1 sq. in. triangle area chosen was simply to facilitate data reduction.

To obtain thickness sensitivity information the teflon triangles were constructed with four different tnicknesses, each thickness consecutively increased by the thickness of the first. The resulting flaw thickness range extended from 6% to 21% of the finished panel thickness.

As the layup process proceeded four teflon triangles, varying in thickness only, were positioned in each of four interlaminar interfaces, as depicted in Fig. 12. By observing the panel from both sides one obtained data for every possible flaw depth.

In order to accurately locate the triangles after the panel had been cured, the triangles were laid on a carefully

measured grid which was marked during layup by embedding 0.002 in. wires in the 0.5 in. border of the panel.

After curing, the panel surfaces were sprayed with flat black enamel. When the enamel had dried, the surfaces were then sprayed with encapsulated cholesteric liquid crystal S-30.

The problem of uniformly heating the panel was approached by mounting the panel in the vertical position in a small vice and attaching the mouth of a large tubular polyurethane plastic bag to the edges of the panel, Fig. 14. The attachment was achieved with long strips of U-shaped plastic molding which left 1.5 in. openings at the corners of the panel. In the other end of the bag was attached a 1.5 in. diameter hose. A smaller perforated plastic bag had previously been attached to the end of the hose so that warm air passing into the larger bag would be effectively diffused. The other end of the hose was connected to a small heater-blower unit capable of heating low velocity air to as high as approximately 70°C.

When the heater-blower unit was switched on, the large bag was slightly pressurized with warm air which soon reached a near steady state condition, thus providing nearly uniform heat over the rear surface of the panel. By observing the front exposed surface, one could detect the color patterns caused by non uniform heat conduction through the panel influenced by the embedded teflon triangles.

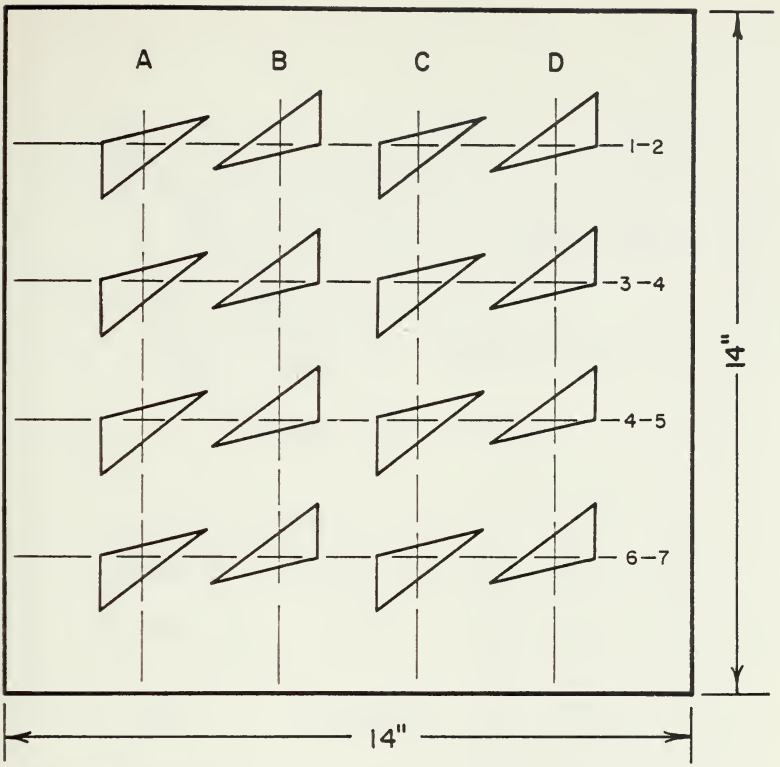

(a) Front view

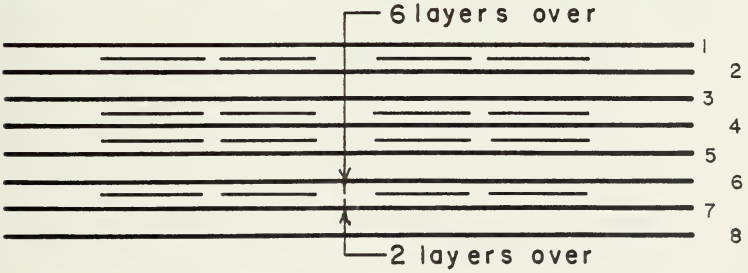

(b) Edge view

Figure 12 - GRAPHITE/EPOXY LAMINATE TEST PANEL

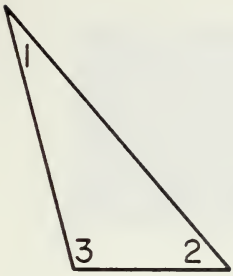

$\angle 1 = 26°$
$\angle 2 = 51°$
$\angle 3 = 103°$

Area = 1.0 in^2

(Shown actual size)

Type	Thickness, in	% d *
A	.009	21.4
B	.0065	15.4
C	.0045	10.7
D	.0025	6.0

* d = finished thickness of panel

Figure 13 - TEFLON TRIANGLES

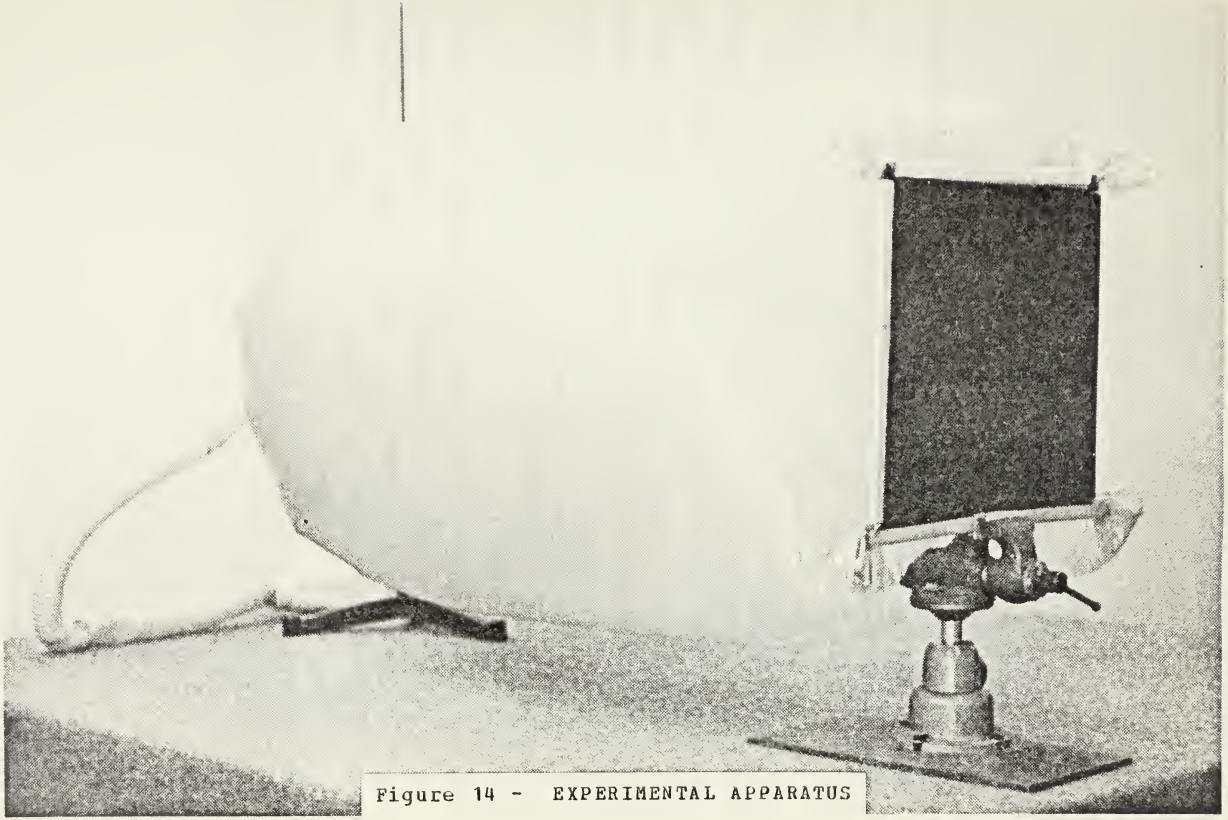

Figure 14 - EXPERIMENTAL APPARATUS

C. RESULTS

With the heating arrangement used it became apparent that holding surface temperatures within a 2°C tolerance at approximately 30°C for the color play zone of the liquid crystals was not possible. However, under the slow transient condition that was actually established, fifteen of the triangles were observed in their undistorted shapes. Since actual flaw detection capability was the primary goal, further attempts to maintain the 2°C tolerance on the surface temperature were not undertaken.

To enhance the location of the thinnest teflon triangles embedded under the most layers, it was necessary to overcome the effects of the different thermal conductivities normal to each other in the panel, which tended to diminish the surface color patterns. Enhancement of the pattern was accomplished by pulsed heating (or cooling) of the local surface above the flaw with an additional heater-blower.

Without sophisicated photographic and printing techniques it was impossible to present black and white photographic results that would accurately represent the subdued surface color patterns that were actually observed. However, the blue and green contrasting pattern most easily observed indicated a degree of sensitivity sufficient to detect the surface temperature difference between areas located above the flawed and unflawed regions within approximately 0.5°C.

V. CONCLUSIONS

It is significant to note that with data from a limited number of test periods it was possible to effectively and consistently obtain order - of - magnitude values for the coefficients of conductivity both normal and parallel to layers in a graphite/epoxy laminate. It is also important to note that without the use of liquid crystals and with the possible substitution of thermocouples for temperature measurement, the procedure for determining the coefficient of conductivity parallel to layers described in part III would be at best extremely difficult. Finally, embedded triangular flaws ranging in thickness from approximately 6 % to 21 % of the total laminate thickness and at every interlaminar depth from one to seven were quite easily detected in undistorted, clearly observable shapes.

In addition to inspection of the panel with intentionally embedded flaws, the pulsed heating technique was successfully employed in another research study to obtain quantative information about impact damage on the same material. Long before normally observable damage had occurred to the graphite/epoxy panels, the pulsed heating technique provided both location and magnitude of the growing damage zone as sequentially increased loads impacted the panel. Only the existence of damage was studied, however, and no attempt was made by this investigator to determine the exact nature of the discontinuities, appearing as a "bruise" early in the impact sequence.

VI. RECOMMENDATIONS

To add to the library of information associated with the family of advanced composites it would be beneficial to fully investigate the transient heat transfer phenomena of the multilayered wall in which the coefficient of conductivity varies with coordinate direction -- the composite laminate panel.

The potential use of encapsulated liquid crystals as an investigative tool, particularly in the inspection of modern composite aircraft components, is great. A particularly beneficial area for investigation would be a correlation of failure prediction, as a result of projectile penetration damage, with theoretically calculable failure orginating from machined holes. An investigation of this nature could ultimately provide the ability to make practical on site damage assessment and repair inspection of aircraft.

Of primary interest was the conceptual design of a device that used the concepts investigated in part IV. Key to the design was the manufacture of a very thin, transparent, heating sheet that would provide a warm contact "foot" on a slightly pressurized clear plexiglass box. A heater of this type was designed and is under construction by MINCO Products, Inc., Minneapolis, Minnesota. Specifications for the 0.005 in. mylar and foil heater are presented in Fig. 15. It is recommended that investigation of the non-destructive testing device pictured in Fig. 16 utilizing the sheet heating element be continued. The proposed device includes a sprayed on layer of liquid crystals and layer of black paint on the outside of the heater sheet, eliminating the need to coat the damaged surface. With airflow through the box, interface contact could be achieved between the surface to be inspected and

the inflated "foot". When the heater was switched on the surface heat would be controlled with a rheostat and while viewing through the clear box one would pulse cold air on the surface, causing rapid transitions through the characteristic event temperature range. Personnel who have only minimal training could perform the inspection using such a device and obtain accurate information on damage to composite aircraft components, inexpensively.

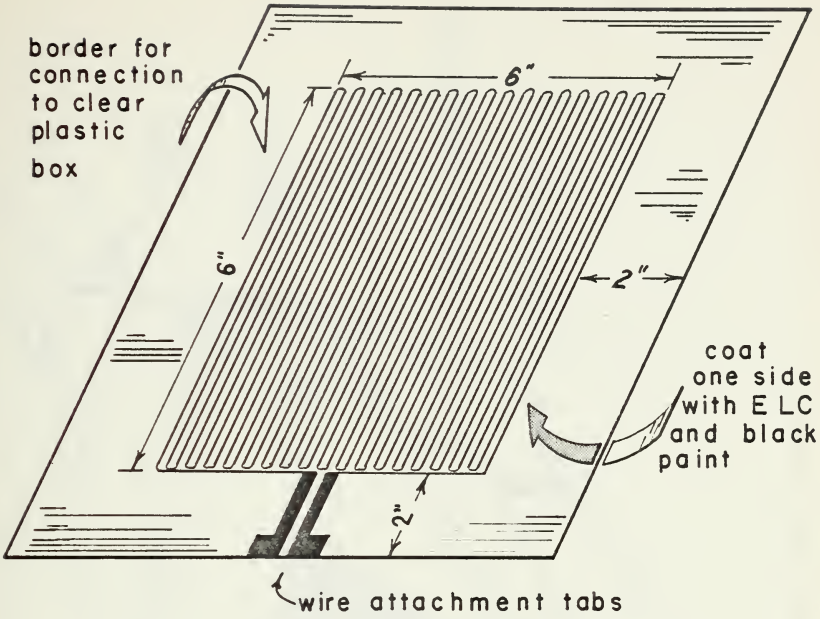

Thickness: finished .005"

Material: etched foil heater
clear mylar film insulator

Lines: .033" wide, .033" spacing

Energy requirements:

deliver 5 watts/in^2

from 156 v, 135 Ω

Figure 15 - DETECTION DEVICE HEATING ELEMENT

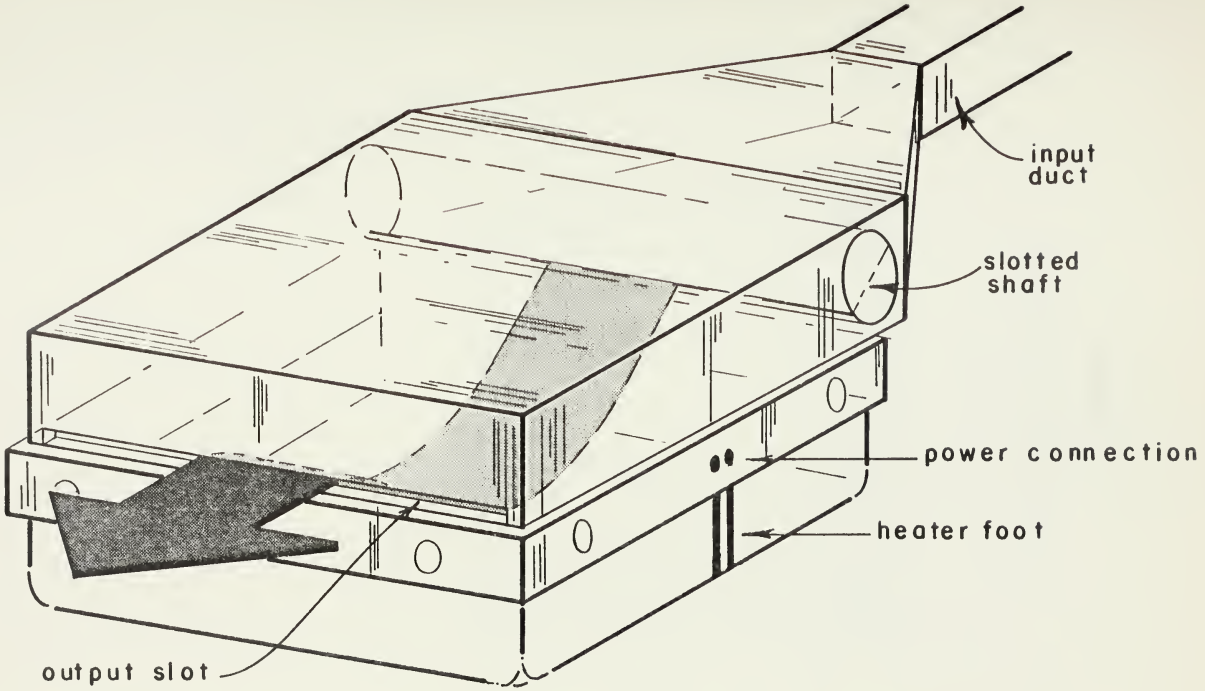

Figure 16 - PROPOSED DETECTION DEVICE

APPENDIX A

CHOLESTERIC LIQUID CRYSTALS

liquid crystal	color transition zones °C red	green	blue
s-30	30.5	31.0	31.6
s-32	32.5	33.1	33.7
s-34	34.7	35.1	35.7
s-36	36.4	36.8	37.4
s-38	38.6	39.1	39.7
s-40	40.6	41.1	41.7
s-43	43.2	43.9	44.6
s-45	45.1	45.6	46.2
s-62	62.2	62.6	63.1

(Summarized from Refs. 13 and 14)

APPENDIX B

MATERIAL PROPERTIES

Specimen discs

Material	k, BTU/h ft °F	thickness in
301 stainless	9.4	.085
Monel	11.3	.050
4130 steel	27.0	.063
7075-T6 aluminum	70.0	.049
Brass	67.7	.041
17-7PH stainless	9.8	.038
Graphite/epoxy 1	----	.038
Graphite/epoxy 2	----	.038
Graphite/epoxy 3	----	.038

Construction materials

Cork	.024
Copper	230
Foam rubber	.01-.02
Hard rubber	.111-.13
Phenolic	.070-.090
Teflon	.150-.175

(Summarized from Refs. 13 and 14)

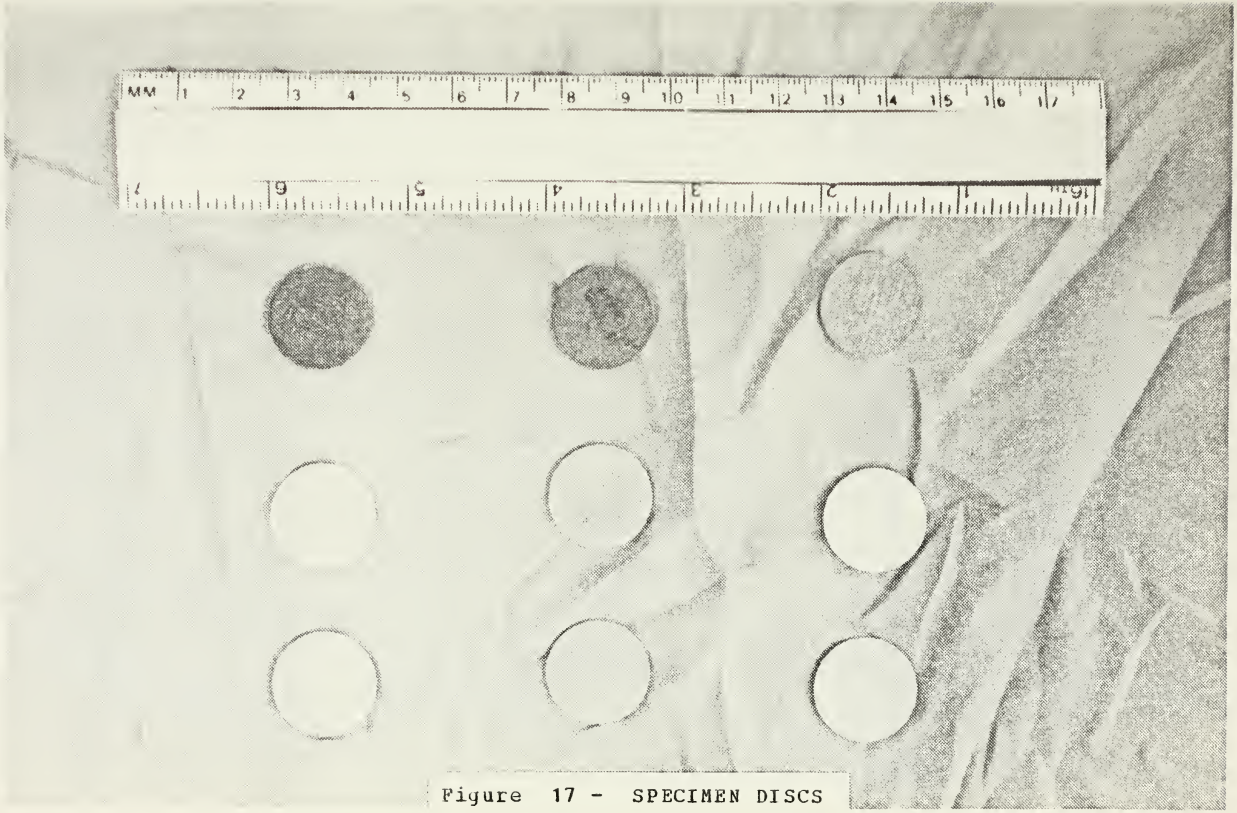

Figure 17 - SPECIMEN DISCS

APPENDIX C

FIN TEMPERATURE DISTRIBUTION

The fins that were tested and subsequently listed in this appendix were all .5 in. wide and .041 in. thick. Their lengths varied as follows:

Brass.....7.27 in.
4130 steel.....7.20 in.
17-7PH stainless..7.27 in.
2024-T3 aluminum..7.22 in.
G/E 1.....6.82 in.
G/E 2.....6.96 in.

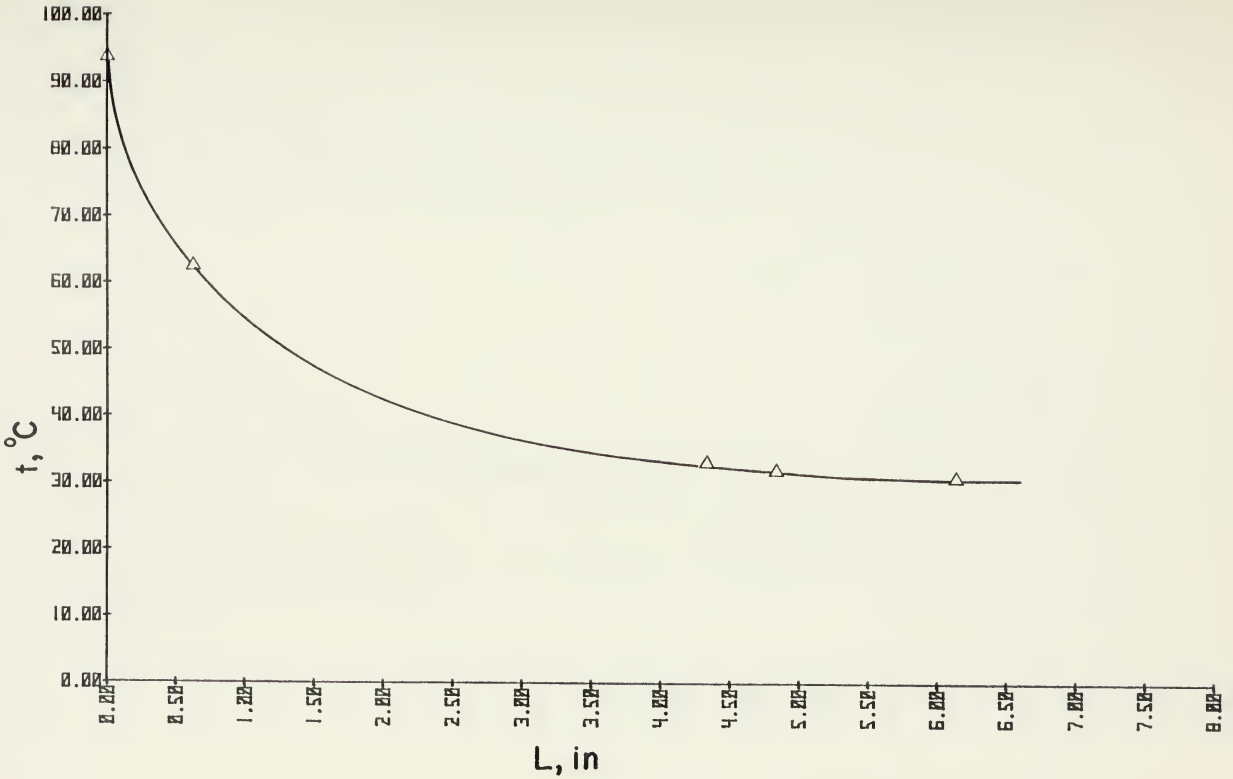

Figure 18 - TEMPERATURE vs. FIN LENGTH, BRASS

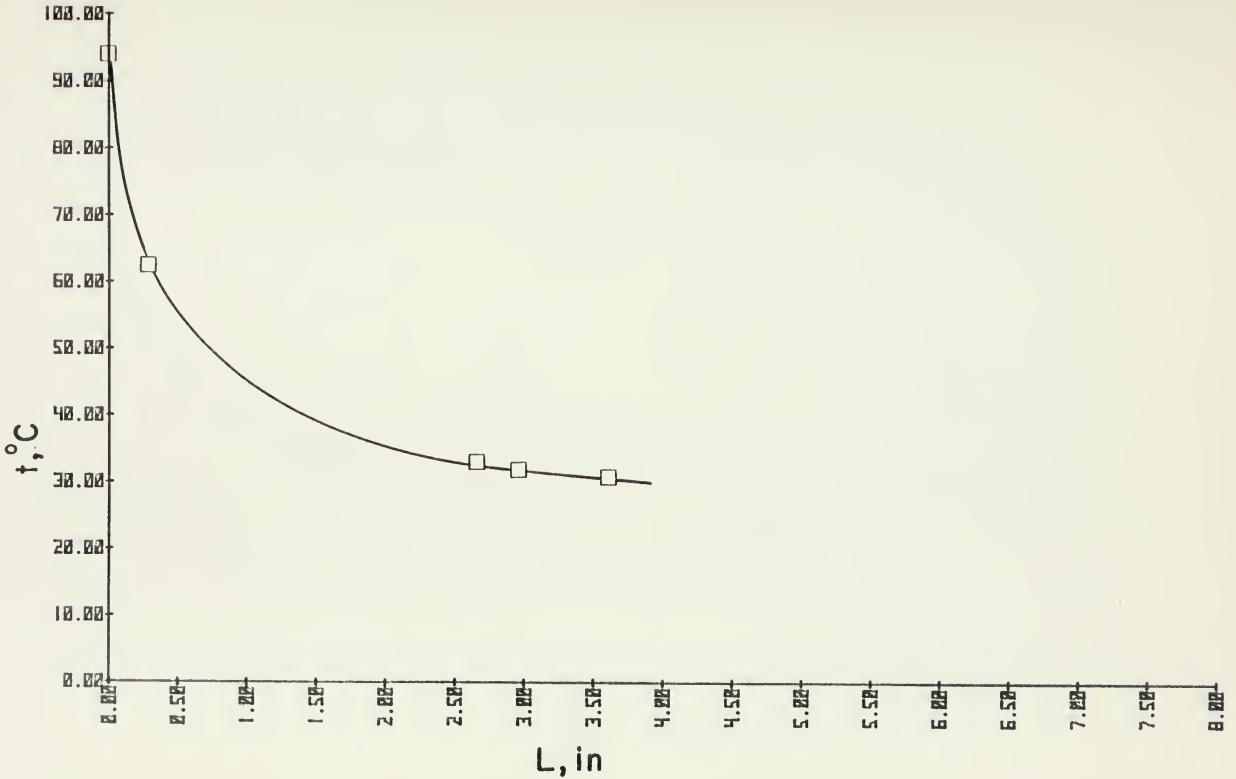

Figure 19 - TEMPERATURE vs. FIN LENGTH, 4130 STEEL

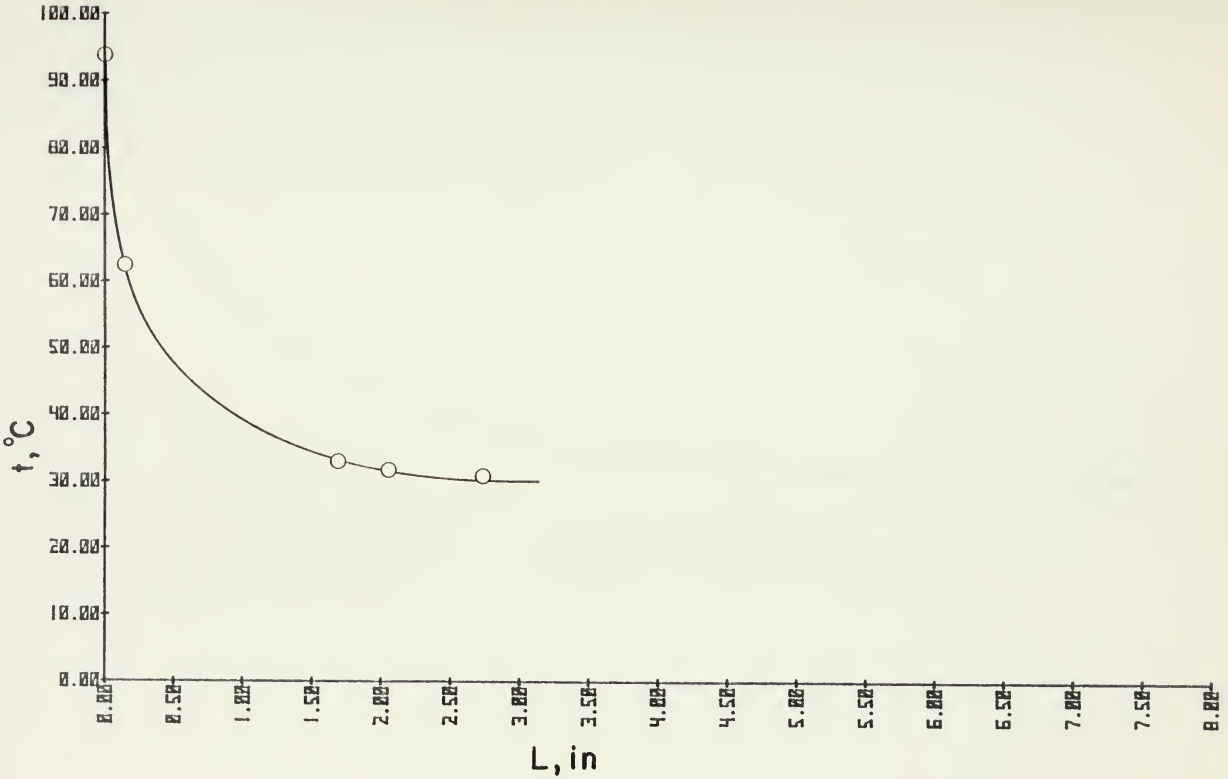

Figure 20 - TEMPERATURE vs. FIN LENGTH, 17-7PH STAINLESS

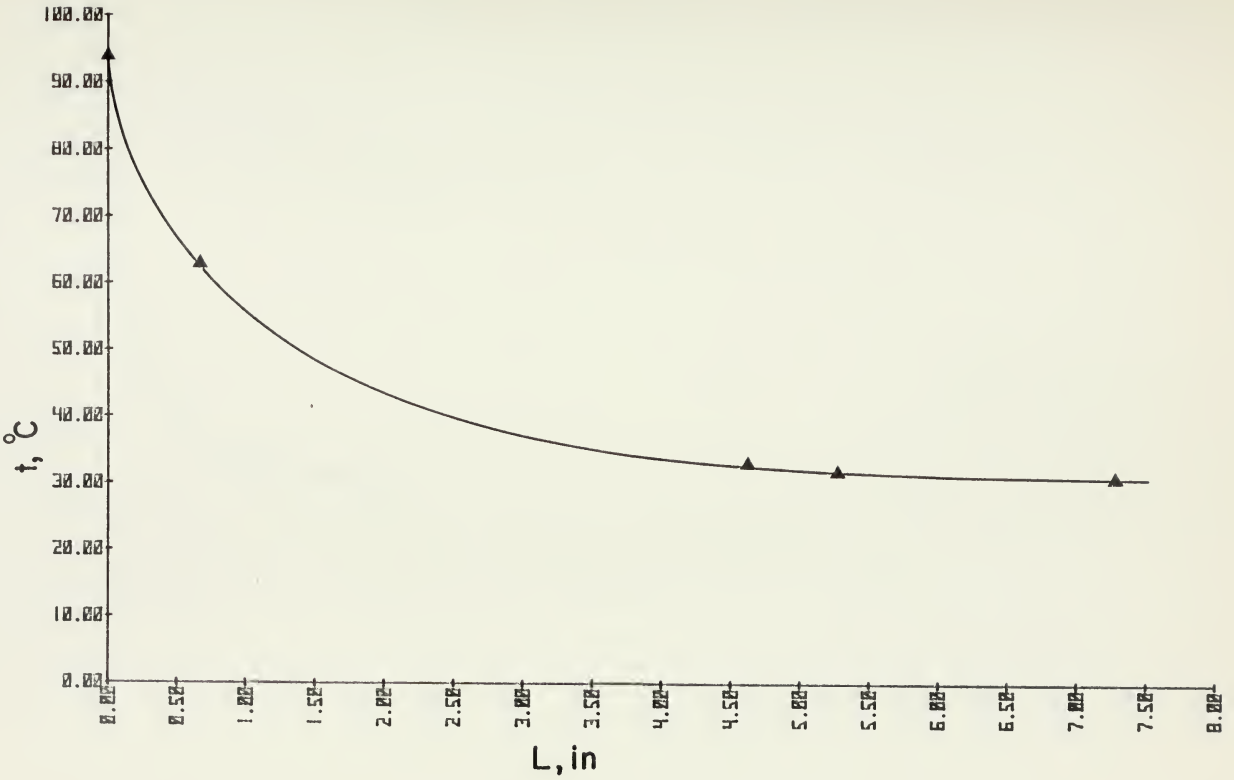

Figure 21 - TEMPERATURE vs. FIN LENGTH, 2024-T3 ALUMINUM

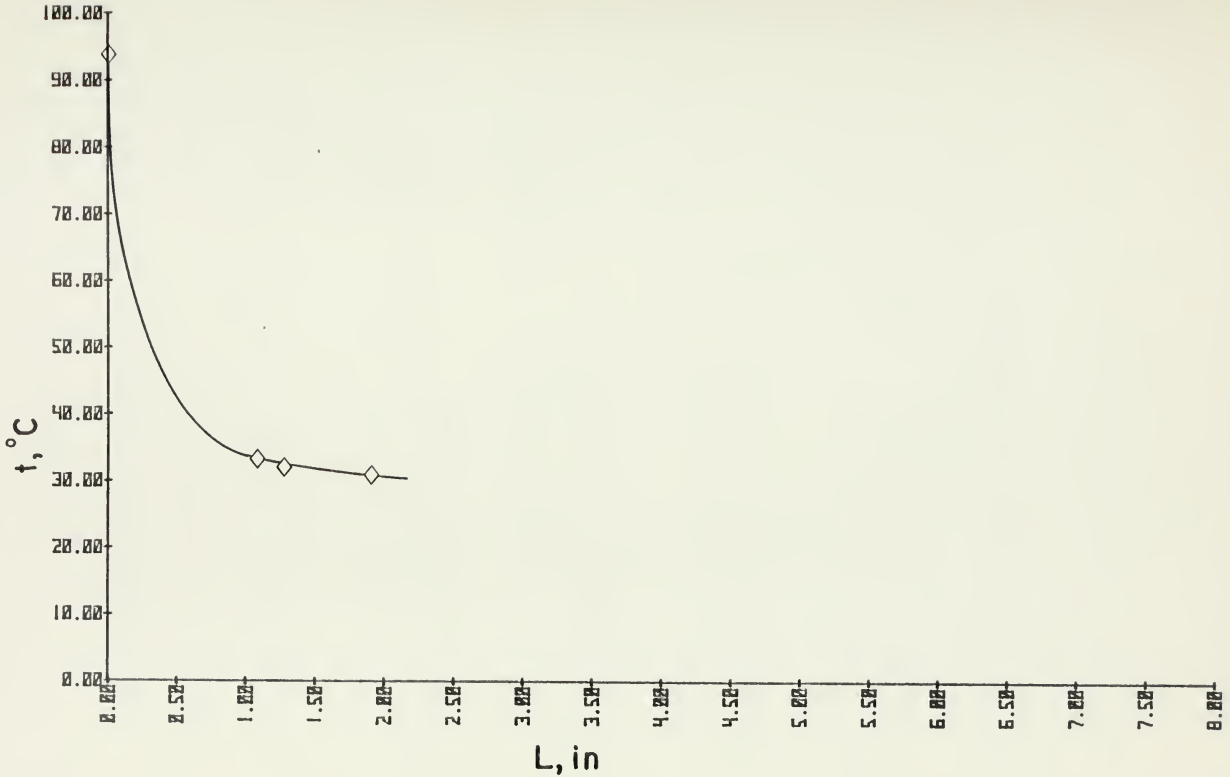

Figure 22 - TEMPERATURE vs. FIN LENGTH, G/E 1

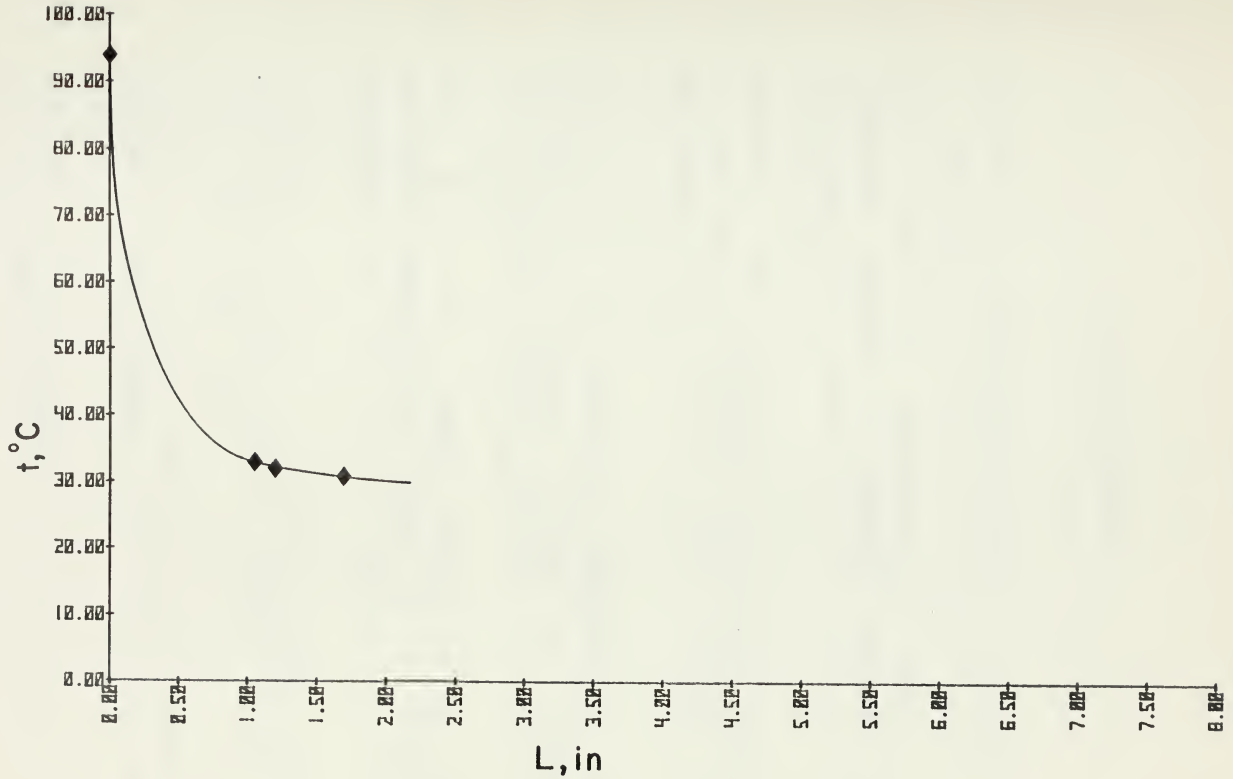

Figure 23 - TEMPERATURE vs. FIN LENGTH, G/E 2

LIST OF REFERENCES

1. NASA SP - 5113, Nondestructive Testing -- A Survey, p. 1 - 268, 1973.

2. AGARD Report 590, Non-destructive Testing and Inspection Applied to Composite Materials and Structures, C.N. Owston and E.H. Jaffe, p. 1 - 31, February 1972.

3. NASA TN D - 7632, Holographic and Ultrasonic Detection of Bond Flaws in Aluminum Panels Reinforced With Boron-Epoxy , R.J. Platt, Jr. and L.B. Thurstin, Jr., p. 1 - 34, July 1974.

4. NASA TR R - 430, Holographic Nondestructive Tests Performed on Composite Samples of Ceramic-Epoxy-Fiberglass Sandwich Structure, R.L. Kurtz and H.K. Liu, p. 1 - 26, June 1974.

5. NASA TP R - 439, Thermal Loading in the Laser Holography Nondestructive Testing of a Composite Structure, H.K. Liu and R.L. Kurtz, p. 1 - 17, May 1975.

6. Woodmansee W. E., " Aerospace Thermal Mapping Applications of Liquid Crystals", Applied Optics, v. 7, p. 1721 - 1729, 1968.

7. Fergason, J. L., "Liquid Crystals in Non-destructive Testing", Applied Optics, v. 7, p. 1729 - 1737, Sept. 1968.

8. Chapman, A.J., Heat Transfer, p. 41 - 46 and 69 - 78, Macmillan, 1974.

9. Holman, J.P., Heat Transfer, p. 35 - 48, McGraw-Hill, 1976.

10. Castellano, J. A., "Thermotropic Liquid Crystals; Part 1. The Underlying Science", Chemical Technology, v. 23, p. 47-52, Jan. 1973.

11. Castellano, J. A., "Thermotropic Liquid Crystals; Part 2. Current Uses and Future Ones", Chemical Technology, v. 29, p. 229-235, Apr. 1973.

12. Cooper, T.E., Field, R.J. and Meyer, J.F. , " Liquid Crystal Thermography and Its Application to the Study of Convective Heat Transfer", Journal of Heat Transfer, v. 99, p. 442 - 450, August 1975.

13. Metals Handbook, 8th ed.,v. 1, pp. 55, 422 - 423, 490, American Society for Metals,1964.

14. Goldsmith, A., Waterman, T. E., and Hirshhorn, H. J., Handbook of Thermophysical Properties of Solid Materials, v. 2, p. 145 - 850, Macmillan Company, 1961.

INITIAL DISTRIBUTION LIST

		No. Copies
1.	Defense Documentation Center Cameron Station Alexandria, Virginia 22314	2
2.	Library, Code 0212 Naval Postgraduate School Monterey, California 93940	2
3.	Department Chairman, Code 67 Department of Aeronautics Naval Postgraduate School Monterey, California 93940	1
4.	Asst Professor Milton H. Bank, Code 67Bt Department of Aeronautics Naval Postgraduate School Monterey, California 93940	5
5.	Lt. Robert T. Schaum, USN 926 Cloverdale Rd. Montgomery, Alabama 36106	1

Thesis
S275 Schaum
c.1
166686
Development of a non-destructive inspection technique for advanced composite materials using cholesteric liquid crystals.